Neoclassical Transport Modeling Compatible with a Two-Fluid Transport Equation System

Mitsuru HONDA, Atsushi FUKUYAMA[1)] and Noriyoshi NAKAJIMA[2)]

Japan Atomic Energy Agency, Naka 311-0193, Japan
[1)]*Graduate School of Engineering, Kyoto University, Kyoto 606-8501, Japan*
[2)]*National Institute for Fusion Science, Toki 509-5292, Japan*

(Received 1 November 2010 / Accepted 17 January 2011)

A neoclassical transport model compatible with a system of two-fluid equations is proposed, with an emphasis on the heat flux contribution. The model is based on the moment approach and is capable of accurately reproducing important neoclassical properties through a simple expression of the neoclassical viscosity tensor, with the aid of the NCLASS module. Applying neoclassical transport theory in a fluid context, we confirm the reproducibility of first-order flows, poloidal flows, neoclassical resistivity, bootstrap current and particle flux.

Keywords: neoclassical transport, neoclassical viscosity, heat flux, two-fluid equation, tokamak

DOI: 10.1585/pfr.6.1403008

1. Introduction

A one-dimensional transport code TASK/TX consisting of two-fluid equations coupled with Maxwell's equations has been developed to investigate the evolution of a plasma self-consistently, including a radial electric field, poloidal and toroidal rotation [1] as well as neutral transport [2]. The code has been applied, for example, in the physics research on toroidal rotation induced by the loss of fast ions due to toroidal field ripple [3] and induced by the charge separation of fast neutrals due to the near-perpendicular NBIs installed in JT-60U [4].

TASK/TX typically solves the continuity equation, the equation of motion in the radial, poloidal and toroidal directions, and the thermal transport equation for electrons and ions respectively, together with Maxwell's equations. The set of equations which TASK/TX solves is essentially different from what a conventional transport code solves, i.e., flux surface-averaged, one-dimensional diffusive transport equations. The chief differences between them are summarized in the following. (1) A conventional code typically calculates particle transport only for ion species due to quasi-neutrality and (2) requires an explicit flux-gradient relationship for a particle flux. (3) It solves a magnetic diffusion equation consistent with Faraday's law, Ampère's law without the displacement current and Ohm's law. (4) It determines poloidal rotation solely as an output using an external neoclassical module and possibly solves a toroidal momentum equation analogous to a thermal transport equation. In contrast, (1) TASK/TX solves the continuity equations for both electrons and ions without explicit quasi-neutrality conditions and (2) also solves an equation of motion in the radial direction, independently. These two differences are also discussed in Ref. [5] in detail. (3) Maxwell's equations are solved to describe the behavior of magnetic fields and electric fields and the evolution of current densities is calculated by solving equations of motion for electrons. (4) Poloidal and toroidal rotations are calculated by solving equations of motion for ions. In that sense, the usual way for incorporating a transport model/module into a conventional transport code cannot be directly adopted with TASK/TX [5].

A similar case holds for neoclassical transport. Neoclassical transport plays a very important role in toroidal plasmas, and, therefore, all chief neoclassical phenomena have to be reproduced in each transport code for toroidal plasmas. Even when we focus only on an ideal axisymmetric plasma, there are many important neoclassical characteristics that must be considered: neoclassical particle and thermal transport, the neoclassical Ware pinch [6], neoclassical resistivity, bootstrap current, neoclassically-driven poloidal flow, the radial electric field and so forth. In conventional transport codes, an external module such as the NCLASS module [7] or the Matrix-Inversion method [8] estimates every quantity corresponding to each neoclassical effect individually, and these quantities are then substituted into an appropriate term in the transport equations: for example, the Ware pinch and particle diffusivity for a particle transport equation; the neoclassical heat pinch and thermal diffusivity for a thermal transport equation; and neoclassical resistivity and bootstrap current for a magnetic diffusion equation. We, therefore, have to invent a method for reproducing all neoclassical effects in a two-fluid TASK/TX system.

These neoclassical transport modules build on the neoclassical moment approach of Hirshman and Sigmar [9]. The moment approach provides a method

author's e-mail: honda.mitsuru@jaea.go.jp

to compute all important neoclassical effects by solving steady-state fluid momentum balance equations in a direction parallel to the magnetic field, with some kinetic treatment, for particle and heat flows. Because these momentum equations are roughly but essentially the same as the equations of motion solved in TASK/TX, we conceived the idea of adding neoclassical viscosity terms to the equations of motion to reproduce neoclassical effects. Hopefully, we will be able to describe self-consistently the neoclassical effects solely by solving the set of two-fluid equations with neoclassical viscosity terms, once we know the neoclassical viscosities.

The poloidal heat flow can drive the poloidal (particle) flow in proportion to the temperature gradient, a fact which will be validated in Sec. 4.3, and this effect may play a significant role in driving the poloidal flow in a plasma with an internal transport barrier. As will be seen in the next section, however, TASK/TX does not include the moment equations for heat flux, implying that it does not reproduce the heat flux-driven poloidal flow within the original framework [1]. As noted in the previous research [3,4], this driving mechanism did not play a key role because plasmas with a moderate temperature gradient were considered. We have to include the heat flux contribution in TASK/TX to fulfil the condition of completeness in neoclassical transport theory and to extend the applicability of the code, by coupling TASK/TX with NCLASS.

We note that neoclassical theory as it relates to the moment approach is found in Refs. [10, 11] in addition to Ref. [9] and it is reviewed particularly well in Ref. [12].

The rest of this paper is organized as follows. Aspects of the basic equations of TASK/TX in association with this study are described in Sec. 2. Analytical investigation demonstrates the existence of first-order flows parallel and perpendicular to the magnetic field in the TASK/TX system, as shown in Sec. 3. Details related to neoclassical transport modeling in TASK/TX are given in Sec. 4, as well as a demonstration of the reproducibility of poloidal flow. Section 5 is devoted to a comparison of neoclassical resistivity and bootstrap current calculated by TASK/TX, NCLASS and the Sauter model [13, 14]. It is demonstrated in Sec. 6 that the radial particle flux can be reproduced accurately. Finally, a summary and discussion are given in Sec. 7.

2. Multi-Fluid Transport Modeling, TASK/TX

We briefly describe the main equations, which become the basis for the following discussion. Currently, the basis equations of TASK/TX essentially build on a concentric circular equilibrium. In this sense, the shaping effects of an equilibrium and the Shafranov shift have not yet been reflected in the code. The following flux surface-averaged quantities for species s are self-consistently solved in the code as the initial boundary value problem: the particle density n_s, the radial flow velocity u_{sr}, the poloidal and toroidal flow velocities $u_{s\theta}$, $u_{s\phi}$. The equations are [1]

$$\frac{\partial n_s}{\partial t} = -\frac{1}{r}\frac{\partial}{\partial r}(r n_s u_{sr}) + S_s, \tag{1}$$

$$\frac{\partial}{\partial t}(m_s n_s u_{sr}) = -\frac{1}{r}\frac{\partial}{\partial r}(r u_{sr} m_s n_s u_{sr}) + \frac{1}{r} m_s n_s u_{s\theta}^2 + e_s n_s (E_r + u_{s\theta} B_\phi - u_{s\phi} B_\theta) - \frac{\partial}{\partial r}(n_s T_s), \tag{2}$$

$$\frac{\partial}{\partial t}(m_s n_s u_{s\theta}) = -\frac{1}{r^2}\frac{\partial}{\partial r}(r^2 u_{sr} m_s n_s u_{s\theta}) + \frac{1}{r^2}\frac{\partial}{\partial r}\left[r^3 m_s n_s \mu_s \frac{\partial}{\partial r}\left(\frac{u_{s\theta}}{r}\right)\right] + e_s n_s (E_\theta - u_{sr} B_\phi) + F_{s\theta}^{\mathrm{NC}} + F_{s\theta}, \tag{3}$$

$$\frac{\partial}{\partial t}(m_s n_s u_{s\phi}) = -\frac{1}{r}\frac{\partial}{\partial r}(r u_{sr} m_s n_s u_{s\phi}) + \frac{1}{r}\frac{\partial}{\partial r}\left(r m_s n_s \mu_s \frac{\partial u_{s\phi}}{\partial r}\right) + e_s n_s (E_\phi + u_{sr} B_\theta) + F_{s\phi}, \tag{4}$$

where m_s and e_s are the mass and charge, respectively. The perpendicular viscosity represents anomalous transport contributions due to turbulent fluctuations. Here, S_s represents the source and sink terms for particles; F_s^{NC}, the force related to neoclassical effects, which will be discussed in detail in the following sections; and $F_{s\theta}$ and $F_{s\phi}$, other forces. In this paper, we do not solve the thermal transport equations, even though they are included in the code. Rather, we fix the temperature profile instead to focus our attention on the neoclassical effects on particles. Maxwell's equations are simultaneously solved using these equations for the evolution of the electromagnetic fields; that is, the radial, poloidal and toroidal electric fields E_r, E_θ, and E_ϕ, and the poloidal and toroidal magnetic fields B_θ and B_ϕ, respectively. Further details of the code are described in Refs. [1–3].

3. First-Order Flow in TASK/TX

In this section, we recall the characteristics of first-order flow in an axisymmetric configuration and then analytically confirm that these characteristics are also inherently present in the TASK/TX system. We intend to demonstrate that it is possible to achieve the results provided solely by using the radial force balance equation, thereby indicating the validity of these results in all collisionality regimes.

3.1 Transport ordering

Neoclassical transport theory relies on an ordering used to categorize transport phenomena based on their magnitude. The basic ordering assumption is that Larmor radius ρ is much smaller than the macroscopic scale length L:

$$\delta \equiv \frac{\rho}{L} \ll 1.$$

The macroscopic scale length L is typically defined by spatial changes in macroscopic parameters, such as pressure.

This ordering is called the small gyroradius ordering, drift ordering or transport ordering. Based on this ordering, we know that the time derivative is considerably smaller:

$$\frac{\partial}{\partial t} \sim O(\delta^2),$$

and the flow velocity V is to first order in δ:

$$V \sim \delta v_{\rm th}.$$

3.2 First-order flow perpendicular to $\boldsymbol{B}$

3.2.1 Theory

In an axisymmetric system, the magnetic field is defined as

$$\boldsymbol{B} = \nabla\phi \times \nabla\psi + I\nabla\phi,$$

where $I(\psi) = RB_\phi$ is a poloidal current and a flux function, a function of the flux surface ψ alone, as well. A fluid moment equation for flow velocity is given by

$$m_s n_s \left.\frac{\mathrm{d}\boldsymbol{u}_s}{\mathrm{d}t}\right|_s = -\nabla p_s - \nabla\cdot\overleftrightarrow{\pi}_s + e_s n_s(\boldsymbol{E}+\boldsymbol{u}_s\times\boldsymbol{B}) + \boldsymbol{R}_s, \quad (5)$$

where $\overleftrightarrow{\pi}_s$ denotes the viscosity tensor and $\boldsymbol{R}_s$, the exchange of momentum. The convective derivative $\mathrm{d}/\mathrm{d}t|_s$ is defined in a frame moving at the fluid velocity $\boldsymbol{u}_s$. Taking the vector product with $\boldsymbol{B}$ from the left, we have to leading order in δ

$$\boldsymbol{u}_\perp \simeq \frac{\boldsymbol{E}\times\boldsymbol{B}}{B^2} + \frac{\boldsymbol{b}\times\nabla p_s}{m_s n_s \Omega_s}, \quad (6)$$

consisting of the $\boldsymbol{E}\times\boldsymbol{B}$ drift and the diamagnetic drift. Here $\boldsymbol{b} \equiv \boldsymbol{B}/B$. The electric field is given by $\boldsymbol{E} = -\nabla\Phi - \partial\boldsymbol{A}/\partial t$, but we now consider only the electrostatic term because to this order the electromagnetic term is negligible. With the aid of the relationship

$$\frac{\boldsymbol{B}\times\nabla\psi}{B^2} = \frac{I}{B}\boldsymbol{b} - R\hat{\phi}, \quad (7)$$

Equation (6) is rewritten as

$$\boldsymbol{u}_{s\perp} = \omega_s\left(R\hat{\phi} - \frac{I}{B}\boldsymbol{b}\right), \quad (8)$$

$$\omega_s \equiv -\frac{\partial\Phi}{\partial\psi} - \frac{1}{e_s n_s}\frac{\partial p_s}{\partial\psi}. \quad (9)$$

Here, $\hat{\phi} = R\nabla\phi$ is the unit vector in the toroidal direction. We call $\boldsymbol{u}_{s\perp}$ a first-order diamagnetic velocity, in accordance with Ref. [10].

3.2.2 TASK/TX

In the TASK/TX system under the assumption of a concentric circular equilibrium, the radial direction is orthogonal to the poloidal direction unlike the straight field-line coordinates. The poloidal direction is geometrically determined, and the magnetic field is expressed as

$$\boldsymbol{B} = B_\theta\hat{\theta} + B_\phi\hat{\phi},$$

where $\hat{\theta}$ is the unit vector in the poloidal direction. From the definition of perpendicular direction, the fluid velocity perpendicular to $\boldsymbol{B}$ is written as

$$\begin{aligned}\boldsymbol{u}_{s\perp} &= \boldsymbol{b}\times(\boldsymbol{u}\times\boldsymbol{b}) \\ &= u_{sr}\hat{r} + \frac{B_\phi}{B^2}(B_\phi u_{s\theta} - B_\theta u_{s\phi})\hat{\theta} \\ &\quad - \frac{B_\theta}{B^2}(B_\phi u_{s\theta} - B_\theta u_{s\phi})\hat{\phi}, \end{aligned} \quad (10)$$

where $\hat{r}$ is the unit vector in the radial direction. The velocity u_{sr} crossing a flux surface is one order smaller than $u_{s\theta}$ and $u_{s\phi}$ and, thus, negligible when we consider the flow to leading order in δ.

Based on the transport ordering, the inertia and centrifugal terms in Eq. (2) are negligibly small and then we obtain

$$B_\phi u_{s\theta} - B_\theta u_{s\phi} \simeq \frac{1}{e_s n_s}\frac{\partial p_s}{\partial r} + \frac{\partial\Phi}{\partial r}. \quad (11)$$

Substituting this force balance relation into Eq. (10) yields

$$\begin{aligned}\boldsymbol{u}_{s\perp} &\simeq (B_\phi u_{s\theta} - B_\theta u_{s\phi})\frac{B_\phi\hat{\theta} - B_\theta\hat{\phi}}{B^2} \\ &= \frac{1}{RB_\theta}\left(-\frac{1}{e_s n_s}\frac{\partial p_s}{\partial r} - \frac{\partial\Phi}{\partial r}\right)\left(-\frac{RB_\theta B_\phi}{B^2}\hat{\theta} + \frac{RB_\theta^2}{B^2}\hat{\phi}\right) \\ &= \omega_s\left(R\hat{\phi} - \frac{I}{B}\boldsymbol{b}\right), \end{aligned}$$

which is identical to Eq. (8), implying that the TASK/TX equation system incorporates the flow perpendicular to $\boldsymbol{B}$. We have used $\partial/\partial\psi \equiv (1/RB_\theta)\partial/\partial r$ in the final step of this derivation.

3.3 First-order flow parallel to $\boldsymbol{B}$

3.3.1 Theory

To leading order in δ, the particle flow is incompressible on a flux surface, while its parallel and perpendicular components are not individually divergence-free due to the inhomogeneity of the strength of the magnetic field along a field line. This characteristic yields a parallel return flow expressed as (see e.g. Sec. 8.5 in Ref. [12])

$$n_s\boldsymbol{u}_{s\parallel} = n_s\frac{I\omega_s}{B}\boldsymbol{b} + K_s\boldsymbol{B}, \quad (12)$$

where K_s is an integral constant and a flux function as well. Taking the scalar product of Eq. (12) with $\nabla\theta$, we find K_s:

$$K_s(\psi) \equiv n_s\hat{u}_{s\theta} = n_s\frac{\boldsymbol{u}_s\cdot\nabla\theta}{\boldsymbol{B}\cdot\nabla\theta}. \quad (13)$$

In fact, K_s/n_s is identical to the contravariant component of the flow, $\hat{u}_{s\theta}$. We note that $\hat{u}_{s\theta}$ does not have a velocity dimension and is also a flux function.

Finally, combining Eq. (8) with Eq. (12), we obtain the first-order particle flow expressed as

$$\boldsymbol{u}_s = \omega_s R\hat{\phi} + \hat{u}_{s\theta}\boldsymbol{B}. \quad (14)$$

When we take the scalar product of $\boldsymbol{u}_s = \boldsymbol{u}_{s\perp} + \boldsymbol{u}_{s\parallel}$ with $\boldsymbol{B}_p = \nabla\phi \times \nabla\psi$, we see the relationship:

$$u_{s\parallel}\frac{\boldsymbol{B}\cdot\boldsymbol{B}_p}{B_p^2} = -B\frac{\boldsymbol{u}_{s\perp}\cdot\boldsymbol{B}_p}{B_p^2} + B\frac{\boldsymbol{u}_s\cdot\boldsymbol{B}_p}{B_p^2}. \tag{15}$$

Obviously, the factor of $u_{s\parallel}$ on the left-hand side (LHS) of the equation is unity and that of B in the second term on the RHS is equivalent to $\hat{u}_{s\theta}$, as seen in Eq. (13). Comparing Eq. (15) to Eq. (12), we have

$$u_{s\parallel} = V_{1s} + \hat{u}_{s\theta}B, \tag{16}$$

$$V_{1s} \equiv -B\frac{\boldsymbol{u}_{s\perp}\cdot\boldsymbol{B}_p}{B_p^2} = \frac{I\omega_s}{B}. \tag{17}$$

In this sense, V_{1s} is the flow along the magnetic field which would cancel the poloidal component of the diamagnetic velocity, $\boldsymbol{u}_{s\perp}$.

A similar case holds for the first-order heat flux parallel to the magnetic field $q_{s\parallel}$, expressed as

$$q_{s\parallel} = \frac{5}{2}p_sV_{2s} + \hat{q}_{s\theta}B, \tag{18}$$

$$V_{2s} = -\frac{I}{m_s\Omega_s}\frac{\partial T_s}{\partial\psi}. \tag{19}$$

$\hat{q}_{s\theta}$ is defined in the same fashion as in Eq. (13).

3.3.2 TASK/TX

The velocity parallel to the magnetic field is obtained by

$$\boldsymbol{u}_{s\parallel} = (\boldsymbol{b}\cdot\boldsymbol{u})\boldsymbol{b} = \frac{B_\theta u_{s\theta} + B_\phi u_{s\phi}}{B}\boldsymbol{b}.$$

With the help of the radial force balance relation in Eq. (11), this expression can be deformed in the following:

$$\begin{aligned} u_{s\parallel} &= \frac{1}{B}\left[\frac{B_\phi}{B_\theta}(B_\theta u_{s\phi} - B_\phi u_{s\theta}) + B_\theta u_{s\theta} + \frac{B_\phi^2}{B_\theta}u_{s\theta}\right] \\ &\simeq \frac{1}{B}\left[-RB_\phi\left(\frac{1}{e_sn_s}\frac{\partial p_s}{\partial\psi} + \frac{\partial\Phi}{\partial\psi}\right) + \frac{u_{s\theta}}{B_\theta}B^2\right] \\ &= \frac{1}{B}\left(I\omega_s + \frac{u_{s\theta}}{B_\theta}B^2\right), \end{aligned} \tag{20}$$

where we have used the definition of ω_s, as given in Eq. (9). Recalling $K_s = n_s\hat{u}_{s\theta} = n_su_{s\theta}/B_\theta$ in a circular concentric equilibrium, we finally have

$$n_s\boldsymbol{u}_{s\parallel} = n_s\frac{I\omega_s}{B}\boldsymbol{b} + n_s\hat{u}_{s\theta}\boldsymbol{B},$$

which is absolutely equivalent to Eq. (12).

4. Neoclassical Transport Modelling Based on the Moment Approach

In order to explain our neoclassical modeling, we briefly recall the moment approach [9] and then demonstrate a mechanism to realize neoclassical effects in the TASK/TX system.

4.1 Neoclassical viscosity tensor

As seen in the derivation of the preceding section, the perpendicular flow in Eq. (8) can be determined uniquely in terms of the thermodynamic forces, while the parallel flow in Eq. (12) cannot because the poloidal flow $\hat{u}_{s\theta}$ is unknown, which is generally a function of the collision frequency. This is also the case for heat flux. In estimating the poloidal flows, we should take into account the neoclassical viscosity term dependent on the collisionality regimes, a term which regulates the behavior of poloidal flows.

Based on the moment approach, using $u_{s\parallel}$ and $q_{s\parallel}$ as given in Eqs. (16) and (18), bearing in mind that there is no first-order parallel viscosity force arising from the ψ derivatives of the flows [10], yields the flux surface-averaged viscosity stress as follows:

$$-\left\langle\boldsymbol{B}\cdot\nabla\cdot\overleftrightarrow{\pi}_s\right\rangle = -3\left\langle(\nabla_\parallel B)^2\right\rangle\left(\mu_{s1}\hat{u}_{s\theta} + \mu_{s2}\frac{2\hat{q}_{s\theta}}{5p_s}\right), \tag{21}$$

$$-\left\langle\boldsymbol{B}\cdot\nabla\cdot\overleftrightarrow{\theta}_s\right\rangle = -3\left\langle(\nabla_\parallel B)^2\right\rangle\left(\mu_{s2}\hat{u}_{s\theta} + \mu_{s3}\frac{2\hat{q}_{s\theta}}{5p_s}\right), \tag{22}$$

where the constant $3\left\langle(\nabla_\parallel B)^2\right\rangle$ has been chosen so that μ_{s1} reduces to Braginskii's classical viscosity coefficient [15] in the collisional limit. Here, $\overleftrightarrow{\theta}_s$ denotes the heat flux tensor analogous to $\overleftrightarrow{\pi}_s$. The unknown coefficients μ_{sj} ($j = 1, 2, 3$) are called neoclassical parallel viscosity coefficients and are expressed as integrals of the velocity dependent viscosities over the velocity space [16]. We adopt in a practical manner the expressions of Eq. (B1) in Ref. [7] and Eq. (20) in Ref. [16] as the viscosities in the banana and Pfirsch-Schlüter regimes, respectively. The chief advantage of this approach is that there is no need to numerically solve any complicated kinetic equations to estimate the neoclassical viscosities.

4.2 Moment equation of neoclassical fluxes

Taking the scalar product of Eq. (5) with $\boldsymbol{B}$ yields to first order in δ

$$-\left\langle\boldsymbol{B}\cdot\nabla\cdot\overleftrightarrow{\pi}_s\right\rangle = -\left\langle B(R_{s\parallel} + e_sn_sE_\parallel^{(A)})\right\rangle, \tag{23}$$

and similarly for the heat flux we have

$$-\left\langle\boldsymbol{B}\cdot\nabla\cdot\overleftrightarrow{\theta}_s\right\rangle = -\left\langle BH_{s\parallel}\right\rangle. \tag{24}$$

Here $E_\parallel^{(A)}$ is the inductive element in the parallel electric field and $H_{s\parallel}$ is a parallel heat friction. These equations constitute the balance equations for momentum and heat. The kinetic treatment of the friction forces $R_{s\parallel}$ and $H_{s\parallel}$ stipulates the relationship between the friction forces and the parallel flows. Therefore, $R_{s\parallel}$ and $H_{s\parallel}$ are expressed by the classical friction coefficients $l_{ij}^{ss'}$ [9] and the parallel flows, and they are valid in all neoclassical regimes.

Substituting the neoclassical viscosity tensors given in Eqs. (21) and (22) and the expressions of the parallel friction forces and the parallel flows given in Eqs. (16) and

(18) into the balance equations given in Eqs. (23) and (24) yields the simultaneous equations in terms of the poloidal flows, expressed as

$$3\left\langle(\nabla_\parallel B)^2\right\rangle\begin{pmatrix}\mu_{s1} & \mu_{s2}\\ \mu_{s2} & \mu_{s3}\end{pmatrix}\begin{pmatrix}\hat{u}_{s\theta}\\ \frac{2\hat{q}_{s\theta}}{5p_s}\end{pmatrix} = \sum_{s'}\begin{pmatrix} l_{11}^{ss'} & -l_{12}^{ss'}\\ -l_{12}^{ss'} & l_{22}^{ss'}\end{pmatrix}\begin{pmatrix} V_{1s}B + \hat{u}_{s'\theta}\left\langle B^2\right\rangle\\ V_{2s}B + \frac{2\hat{q}_{s'\theta}}{5p_{s'}}\left\langle B^2\right\rangle\end{pmatrix} + \begin{pmatrix} e_s n_s\left\langle E_\parallel^{(A)}B\right\rangle\\ 0\end{pmatrix}. \quad (25)$$

Once the inductive parallel electric field $E_\parallel^{(A)}$ is known, solving the simultaneous equations yields the poloidal flows and subsequently the particle and heat flows in the parallel direction. Roughly speaking, Eq. (25) includes the equations that are practically solved in NCLASS.

4.3 Qualitative interpretation of neoclassical flows

It is meaningful to focus on the relationship between neoclassical viscosities and flows by considering the limit to a large aspect ratio, $\epsilon \ll 1$. In this limit, the viscosities μ_{sj} are generally much smaller than the friction forces $l_{ij}^{ss'}$, and subsequently the ratio of the former to the latter can be used as a small expansion parameter [9,10]. Neglecting the $E_\parallel^{(A)}$ contribution, to lowest (zeroth) order in the ratio, we have $\langle BR_{s\parallel}\rangle = 0$ and $\langle BH_{s\parallel}\rangle = 0$. Momentum conservation in Coulomb collisions guarantees that the friction forces depend solely on relative parallel particle flows. Therefore, the solutions to Eqs. (16), (18) and (25) must have the form: $\langle u_{s\parallel}B\rangle \simeq \langle VB\rangle$ and $\langle q_{s\parallel}B\rangle \simeq 0$. The former result indicates that all species have a common flow equal to $\langle VB\rangle$ to lowest order in the ratio.

Based on $\langle BR_{s\parallel}\rangle = 0$ and quasi-neutrality, summing Eq. (23) over all species including electrons yields $\sum_s\left\langle \boldsymbol{B}\cdot\nabla\cdot\overleftrightarrow{\pi}_s\right\rangle = 0$. Substituting the parallel flows given in Eqs. (16) and (18) and the neoclassical viscosity term given in Eq. (21) into this equation, we have after averaging it over the flux surface and summing it over all species

$$\langle VB\rangle = \frac{\sum_s(\mu_{s1}\langle V_{1s}B\rangle + \mu_{s2}\langle V_{2s}B\rangle)}{\sum_s \mu_{s1}}.$$

Because electron neoclassical viscosity is in general smaller by a factor of $(m_e/m_i)^{1/2}$ than ion viscosity, the common flow V is almost exclusively governed by ion motion.

For instance, considering a pure plasma consisting only of electrons and ions without impurities, the ion poloidal flow is expressed as

$$\hat{u}_{i\theta} = \frac{1}{\langle B^2\rangle}(\langle VB\rangle - \langle V_{1s}B\rangle) = \frac{1}{\langle B^2\rangle}\frac{\mu_{i2}}{\mu_{i1}}\langle V_{2i}B\rangle = -\frac{\mu_{i2}}{\mu_{i1}}\frac{I}{Z_i e\langle B^2\rangle}\frac{\partial T_i}{\partial\psi}, \quad (26)$$

applying Eq. (19). This form provides an important result: poloidal flow is proportional to the temperature gradient via the neoclassical viscosities. Usually there is a finite and negative temperature gradient in a plasma, such that the poloidal flow is always driven by the temperature gradient, owing to the heat flux contribution, μ_{i2}. If the contribution from the heat flux to the momentum were ignored, i.e., $\mu_{i2} = 0$, the poloidal flow would never be neoclassically driven and would just be damped due to the neoclassical viscosity μ_{i1} at some point, as clearly seen in Eq. (21). Physically, the damping of the poloidal flow in connection with the first term in parentheses in Eq. (21) is due to collisions between trapped particles and passing particles.

4.4 Implementation of the neoclassical viscosity term in TASK/TX

In a perfect axisymmetric tokamak, there are no neoclassical viscosities working in the toroidal direction, based on standard neoclassical theory. Roughly speaking, toroidal flow may be balanced by an external torque input and transport of momentum, free from neoclassical transport: this fact will be discussed in detail in another paper. In fact, we found that the neoclassical moment approach builds on the equation of motion in a direction parallel to $\boldsymbol{B}$, as seen in the preceding sections, and the equation of motion in the toroidal direction has nothing to do with the moment approach.

A parallel equation of motion is developed in the TASK/TX system by summing the poloidal equation of motion given in Eq. (3), multiplied by B_θ and the toroidal equation of motion given in Eq. (4), multiplied by B_ϕ. Considering the above statements, we find that we should include the neoclassical viscosity tensor only in the poloidal equation of motion as follows:

$$F_{s\theta}^{NC} \equiv -\frac{1}{B_\theta}\left\langle \boldsymbol{B}\cdot\nabla\cdot\overleftrightarrow{\pi}_s\right\rangle = -\frac{\left\langle B^2\right\rangle}{B_\theta}\frac{3\left\langle(\nabla_\parallel B)^2\right\rangle}{\langle B^2\rangle}\left(\mu_{s1}\frac{u_{s\theta}}{B_\theta} + \mu_{s2}\frac{2\hat{q}_{s\theta}}{5p_s}\right), \quad (27)$$

where we have used $\hat{u}_{s\theta} = u_{s\theta}/B_\theta$ as valid in the TASK/TX system. In a practical sense, TASK/TX uses the NCLASS module [7] to calculate the neoclassical viscosities, given as $3\left\langle(\nabla_\parallel B)^2\right\rangle\mu_{sj}/\left\langle B^2\right\rangle$, where $j = 1, 2$, and the poloidal heat fluxes, given as $2\hat{q}_{s\theta}/5p_s$. TASK/TX solves the momentum equations for the particles given in Eqs. (2), (3) and (4) but never solves the momentum equations for heat. In this sense, $u_{s\theta}$, appearing in the first term in the parentheses of Eq. (27), can be calculated as one of the dependent variables by solving the set of equations in TASK/TX, while $\hat{q}_{s\theta}$ in the second term, stemming from the momentum equations for heat, cannot be determined solely within the current framework of TASK/TX. Therefore, at present, the poloidal heat flux $\hat{q}_{s\theta}$ is estimated by NCLASS: we would like to emphasize that this is essentially the only variable for which NCLASS is used for subsequent calculations in TASK/TX. We finally note that we may regard our model as proposed here to be a combination of the ba-

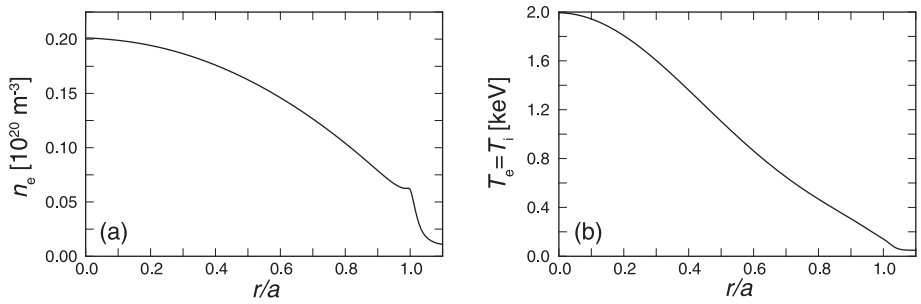

Fig. 1 Background radial profiles of (a) the electron density and (b) the electron and ion temperatures.

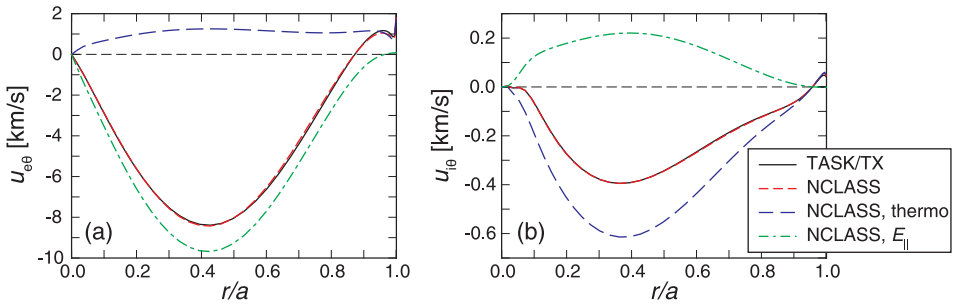

Fig. 2 Comparison of the poloidal flow for (a) electrons and (b) ions. The short broken line in red (NCLASS) is the sum of the long broken line in blue (NCLASS, thermo) and the chain line in green (NCLASS, $E_{\|}$).

sis equations of TASK/TX and Eq. (25), because $\hat{q}_{s\theta}$ is estimated in NCLASS by solving Eq. (25), in practice.

4.5 Comparison of the poloidal flow

As expected from the discussion in Sec. 4.2, NCLASS implemented in TASK/TX also provides $\hat{u}_{s\theta} = u_{s\theta}/B_\theta$, as well as $\hat{q}_{s\theta}$. Accordingly, we can directly compare the poloidal flow $u_{s\theta}$ as a dependent variable in TASK/TX to $\hat{u}_{s\theta}$ as calculated directly in NCLASS. In other words, we compare the solution of Eq. (3) to that of Eq. (25), in terms of the poloidal flow.

Plasma parameters comparable to the JT-60U's are used: the major radius $R = 3.2$ m, the minor radius $a = 0.8$ m, the toroidal field $B_{T0} = 3.2$ T, and the plasma current $I_p = 0.6$ MA. The profiles of n_e, T_e and T_i are shown in Fig. 1. Temperature profiles are fixed throughout the simulation. We consider a pure plasma consisting of electrons and ions only: the effective charge $Z_{eff} = 1.0$. Focusing on neoclassically-driven poloidal flow, we set the anomalous particle diffusivity to zero. This choice stems from the fact that in TASK/TX modeling, an anomalous particle flux is achieved through a change in the poloidal force due to turbulence [5].

A comparison of the poloidal flow for electrons and ions calculated by TASK/TX and NCLASS, respectively, is shown in Fig. 2 and indicates very good agreement for both cases. This finding means that the neoclassically-driven poloidal flow clearly can be reproduced in the TASK/TX system, following the introduction of Eq. (27). NCLASS also provides each component of the total poloidal flow. Figure 2 (a) shows that the electron poloidal flow is dominated by the contribution from the parallel electric field $E_{\|}$, while Fig. 2 (b) shows that the ion poloidal flow is mainly governed by the thermodynamic forces proportional to the gradients of temperature and pressure, stemming from the heat flux contribution. In this sense, the heat flux contribution to the particle flux is essential for accurately reproducing the neoclassical effects in the two-fluid modeling.

Even if many terms, such as anomalous perpendicular diffusion, classical collision, collision with neutrals, and charge exchange loss, are included in Eq. (3), the resultant poloidal flow is identical to the one estimated by NCLASS. In other words, the neoclassical viscosity tensor plays a dominant role in determining poloidal flow. In contrast, a force model producing a quasilinear particle flux due to turbulence [5], implemented in TASK/TX, could alter poloidal flow from a purely neoclassical poloidal flow, if it were activated. It is natural, however, that turbulence influences neoclassical characteristics as analytically elucidated by Shaing [17].

The neoclassical modeling of TASK/TX given in Eq. (27) has many advantages. First of all, this modeling never intervenes in the two-fluid equation system; it simply requires the neoclassical viscosity term to be added to the poloidal equation of motion. Secondly, an additional effect can be readily included in this framework. For example, we have a new equilibrium state of the poloidal

flow that stems from both the neoclassical and additional effects when we add a torque source other than neoclassical transport. This feature will be useful to investigate the behavior of experimentally observed poloidal flow that deviates from neoclassical predictions [18]. Thirdly, this modeling is compatible with self-consistent modeling in terms of the evolution of the polarization current. TASK/TX has been applied to the study of E_r and toroidal rotation driven by an ambipolar radial current created by NBIs [3, 4]. These studies can be conducted using the feature of TASK/TX which solves the poloidal equation of motion with Maxwell's equations: the evolution of E_r is neoclassically linked to that of the radial (polarization) current through that of the poloidal flow. This neoclassical modeling can reproduce the above important neoclassical characteristics of a plasma without violating the current framework of TASK/TX. The relationship between E_r and the radial current will be discussed in detail in another paper.

5. Reproducibility of Neoclassical Resistivity and Bootstrap Current

Two important neoclassical characteristics are neoclassical resistivity and bootstrap current, the former of which regulates the penetration time of an ohmic current and the latter of which is the sole, self-generating (bootstrap) current in a plasma without an external drive and is expected to play an indispensable role in a steady-state, non-inductive plasma. All transport codes for a plasma in a tokamak must take both effects into account.

Because TASK/TX tracks the current evolution as electron motion by solving the equations of motion for electrons, resistivity and bootstrap current do not explicitly appear in the set of equations, unlike conventional diffusive transport codes. These effects are naturally embedded in the total current density; hence, the only result evident in the solution of these equations is the total current density in the radial, poloidal and toroidal directions, i.e., the radial electron flux and the parallel and toroidal current densities. We anticipate that these effects would appear solely by introducing the neoclassical viscosity tensor given in Eq. (27) into the set of equations. Therefore we should confirm whether the viscosity term produces neoclassical resistivity and bootstrap current in TASK/TX through some other means.

In order to validate the TASK/TX results, we extract the components associated with resistivity and bootstrap current from analytically-reduced formulae for the set of basis equations of TASK/TX. In this respect, the comparison has been already carried out in Ref. [1]. However, the neoclassical contribution from the heat flux to the particle flux was not included at that point; hence, in some sense the comparison was incomplete. In this section, we approximately formulate a steady-state analytical solution of the equations for electrons, and after extracting corresponding terms from the steady-state flux, we compare them with those from NCLASS and the Sauter model, briefly explained below, in a manner similar to that in Ref. [1].

5.1 Theoretical models

5.1.1 NCLASS

NCLASS, which calculates the neoclassical viscosities and the heat flux used in TASK/TX, is also capable of determining neoclassical resistivity and bootstrap current. Specifically, the former is figured directly by NCLASS; the latter is derived, as follows, from thermodynamic gradients and the NCLASS-supplied coefficients:

$$\langle j_{\parallel \mathrm{BS}} B \rangle = \sum_s \left(C^{\mathrm{BS}}_{T,s} \frac{T'_s}{T_s} + C^{\mathrm{BS}}_{p,s} \frac{p'_s}{p_s} \right), \tag{28}$$

where s is the species and the prime denotes the ψ-derivative.

5.1.2 Sauter model

The CQLP code [19], solving the Fokker-Planck equation with a full collision operator and including variation along the magnetic field line, coupled with adjoint function formalism, is used to calculate coefficients for resistivity and bootstrap current in arbitrary equilibrium and collisionality regimes. The results for a wide range of plasma parameters are applied to model-fitted formulae, termed the Sauter model [13, 14]. The model distinguishes itself from NCLASS in terms of its fast calculation speed due to the algebraic formulae and highly accurate estimates due to a full-collision operator: the moment approach without the full-collision operator may cause errors up to 20% [7].

The Sauter model does not include the effects of potato orbit particles. Also, it cannot estimate anything neoclassical other than neoclassical resistivity and bootstrap current, meaning that it alone does not include all variables regarding neoclassical effects, unlike NCLASS.

5.2 Analytical estimation in TASK/TX

As shown in Sec. 2.3 of Ref. [1], we may reduce the set of equations to obtain analytical expressions of electron flows by assuming a steady state and neglecting relatively small factors and ion flows.

Because neoclassical resistivity $\eta_\parallel$ is determined by the equation $j_\parallel = \eta_\parallel^{-1} E_\parallel$, terms proportional to $E_\parallel$ should be extracted from electron steady-state fluxes in the poloidal and toroidal directions. The electron parallel current can be written as

$$j_\parallel = -e n_\mathrm{e} \frac{B_\phi u_{\mathrm{e}\phi} + B_\theta u_{\mathrm{e}\theta}}{B}. \tag{29}$$

After analytically estimating the steady-state poloidal and toroidal fluxes for electrons, we substitute terms proportional to $E_\parallel$ in the $u_{\mathrm{e}\theta}$ and $u_{\mathrm{e}\phi}$ equations into Eq. (29) to

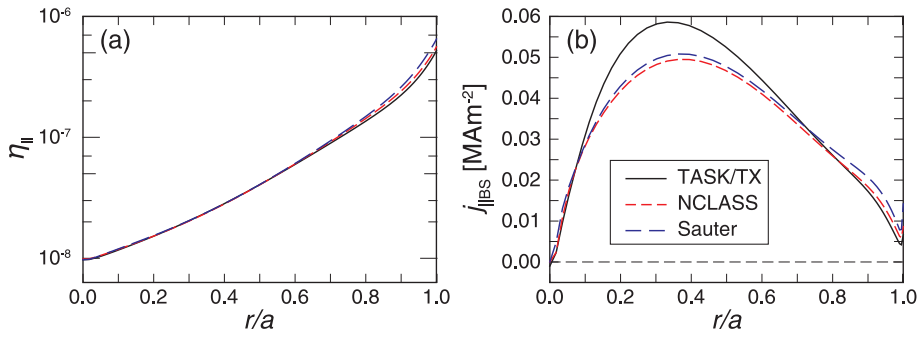

Fig. 3 Comparison of TASK/TX using Eqs. (31) and (33), NCLASS and the Sauter model for estimates of (a) neoclassical resistivity and (b) bootstrap current.

obtain

$$j_{\parallel} = \frac{e^2 n_e}{m_e \bar{\nu}_3} \frac{1}{1+\alpha} \frac{B^2}{B_\phi^2} \left(1 + \frac{B_\theta}{B} \frac{F^q_{e\theta}|_{E_\parallel}}{e n_e}\right) E_\parallel, \tag{30}$$

where $\bar{\nu}_3$ is the contribution from the classical collision and α is the non-dimensional parameter dependent on classical and neoclassical collisionalities, both of which are defined in Ref. [1]. The heat flux contribution $F^q_{e\theta}|_*$ is expressed as

$$F^q_{e\theta}|_* = \frac{3\left\langle (\nabla_\parallel B)^2 \right\rangle}{B_\theta} \mu_{e2} \frac{2\hat{q}_{e\theta}}{5p_e}\bigg|_*,$$

where the subscript $*$ denotes the component of the heat flux associated with a quantity "$*$": $E_\parallel$, in this case. Substituting $F^q_{e\theta}|_{E_\parallel}$ into Eq. (30) and dividing it by $E_\parallel$ yield

$$\eta_\parallel = \frac{m_e \hat{\nu}_3 (1+\alpha)}{e^2 n_e} \frac{B_\phi^2}{B^2} \left(1 + \frac{3\left\langle (\nabla_\parallel B)^2 \right\rangle}{B E_\parallel} \frac{\mu_{e2}}{e n_e} \frac{2\hat{q}_{e\theta}}{5p_e}\bigg|_{E_\parallel}\right)^{-1}, \tag{31}$$

where $E_\parallel$ in the denominator in parentheses may be offset by $E_\parallel$ implicitly appearing in the heat flux contribution $\hat{q}_{e\theta}$, indicating that $\eta_\parallel$ does not explicitly depend on $E_\parallel$.

In the classical limit, $(1+\alpha)\bar{\nu}_3 \approx \nu_{ei\parallel} B^2/B_\phi^2$, and the heat flux contribution becomes nil. Subsequently, Eq. (31) is reduced to

$$\eta^{cl}_\parallel = \nu_{ei\parallel} \frac{m_e}{e^2 n_e} \equiv N(Z_{eff}) \nu_{ei} \frac{m_e}{e^2 n_e}, \tag{32}$$

where ν_{ei} is the electron-ion collision frequency and $N(Z_{eff})$ is the correction function of the collision frequency with respect to the effective charge Z_{eff}, which takes into account the electron-electron collision effect [9]: In a pure plasma with $Z_{eff} = 1$, $N(1) \approx 0.51$. We, therefore, find that Eq. (32) recreates the classical resistivity.

A similar case holds for bootstrap current. Bootstrap current consists of terms proportional to the pressure and temperature gradients, p' and T', typically rendered as in Eq. (28). The p'-driven current originates from the diamagnetic drift, and the T'-driven current originates from the heat flux. In this sense, we have to include the T' contribution calculated by NCLASS in order to estimate bootstrap current. Substituting terms proportional to p' and T' in the $u_{e\theta}$ and $u_{e\phi}$ equations into Eq. (29) yields

$$j_{\parallel BS} = -\frac{1}{(1+\alpha)\bar{\nu}_3 B_\phi} \left(\frac{B_\theta}{B} \nu_{NCe} \frac{\partial p}{\partial r} - \frac{B B_\theta}{B_\phi} \frac{e F^q_{e\theta}|_{T'}}{m_e}\right), \tag{33}$$

where p is the total pressure. The expression of $F^q_{e\theta}|_{T'}$ has already been defined above. We should emphasize that we have imposed a rough assumption in this derivation in that we have ignored the contributions of ion flows. We will discuss the influence of neglecting the contribution of ions to bootstrap current in the last part of the next section.

5.3 Comparison of neoclassical resistivity and bootstrap current

The simulation conditions used are identical to those given in Sec. 4.5. We compare neoclassical resistivity and bootstrap current estimated by TASK/TX, NCLASS and the Sauter model. We use Eq. (31) as the neoclassical resistivity model and Eq. (33) as the bootstrap current model for TASK/TX. Good agreement on neoclassical resistivity $\eta_\parallel$ is obtained with these three models, as shown in Fig. 3 (a). Especially, resistivity calculated by NCLASS is nearly equivalent to that estimated by TASK/TX. Considering that the neoclassical framework of TASK/TX builds on the moment approach adopted in NCLASS, the fact that the results from both are nearly identical demonstrates that TASK/TX could incorporate the moment approach internally. The slight difference in $\eta_\parallel$ between the Sauter model and the others may be ascribed to the approach to modeling, i.e., a fitted formula based on Fokker-Planck analyses and the moment approach.

Also, agreement on bootstrap current is obtained, as shown in Fig. 3 (b). A slight deviation of the TASK/TX estimation from the others is observed in the core region, but the maximum deviation falls within a factor of 1.2. When we compare the deviation in Fig. 3 (b) to a peak of the $u_{i\theta}$ profile in Fig. 2 (b), we deduce that the deviation of bootstrap current has to do with the shape of the ion poloidal flow $u_{i\theta}$. Actually, the location of the maximum deviation may be linked to that of the maximum magnitude in $u_{i\theta}$. This finding leads to the deduction that neglecting the con-

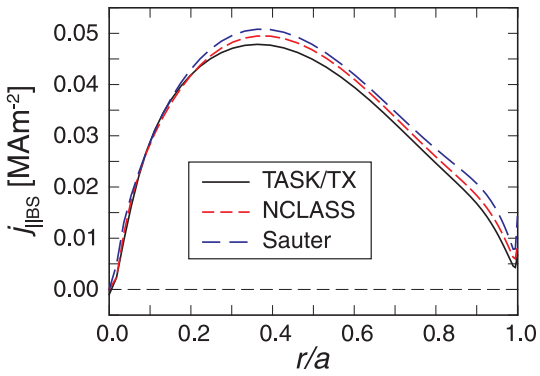

Fig. 4 Comparison of TASK/TX using Eq. (34), NCLASS and the Sauter model for estimates of bootstrap current. The figure indicates that the contribution of the ion poloidal flow to the bootstrap current as included in Eq. (34) is significant.

tribution of ion flows produces the deviation, a deduction supported by the fact that the current is the sum of the electron and ion flows.

In this case, no significant ion toroidal flow exists because an external torque is not applied to the plasma; only poloidal flow may exert an impact on bootstrap current. We extend the approximate expression of bootstrap current given in Eq. (33) so as to include the contribution from $u_{i\theta}$, as follows:

$$j_{\|BS} = -\frac{1}{(1+\alpha)\bar{\nu}_3 B_\phi}\left[\frac{B_\theta}{B}\nu_{NCe}\frac{\partial p}{\partial r} - \frac{BB_\theta}{B_\phi}\frac{eF^{q}_{e\theta}|_{T'}}{m_e} - \left(\frac{B_\theta B_\phi}{B}\nu_{NCe} - B\nu_{ei\|}\right) en_e u_{i\theta}\right]. \quad (34)$$

We use a self-consistent solution of $u_{i\theta}$ calculated by TASK/TX, when estimating bootstrap current using Eq. (34). Figure 4 shows a comparison of bootstrap current among Eq. (34), NCLASS and the Sauter model: Eq. (34) reproduces quite accurately the bootstrap current estimated by NCLASS as well as the Sauter model. This finding means that the deviation in Fig. 3 (b) is in large measure ascribed to neglecting ion poloidal flow. This result also supports our contention that the neoclassical properties of resistivity and bootstrap current can be reproduced accurately in the TASK/TX system.

Finally, we note that Eq. (34) is not quite appropriate as an approximate formula of bootstrap current because the poloidal "flow" $u_{i\theta}$ is explicitly included to describe the current "flow". Ideally, we should have replaced $u_{i\theta}$ in Eq. (34) with terms not directly including the flows. However, it is quite difficult to analytically reduce the set of equations of TASK/TX to a set of approximate, linear formulae for all dependent variables. We, therefore, opt for the second best way to describe bootstrap current as in Eq. (34) by numerically calculating $u_{i\theta}$.

6. Reproducibility of Neoclassical Particle Flux

Basically, neoclassical transport in terms of particles and heat is much smaller than turbulent transport. Cross-field transport, with a step size typically similar to a banana width, is on the order of $O(\delta^2)$, which is also much smaller than parallel, poloidal and toroidal flows. One of the important neoclassical transport properties is the Ware pinch [6], which is directed inward as long as $E_\|$ exists and may lead to a peaked density profile towards the magnetic axis.

As is clear in Eqs. (1) and (2), there are no explicit neoclassical convection and diffusion terms in the equations associated with particle transport. As such, we should clearly demonstrate that neoclassical particle transport does occur in the TASK/TX system through the neoclassical viscosity tensor given in Eq. (27), as is the case with the other neoclassical properties mentioned above. In this section, we confirm the existence of neoclassical particle transport in our neoclassical modeling and then compare the particle flux with that directly estimated by NCLASS.

6.1 Radial particle flux

First of all, let us recall how the cross-field radial particle flux Γ_{si} is derived in neoclassical transport theory. By derivation, we omit the subscript i meaning charge state, for the sake of simplicity. Considering the flux surface-averaged toroidal projection ($R\hat{\phi}$) of the equation of motion given in Eq. (5), we have

$$\langle \boldsymbol{\Gamma}_s \cdot \nabla\psi \rangle = -\frac{1}{e_s}\left\langle R(R_{s\phi} + e_s n_s E^{(A)}_\phi)\right\rangle,$$

where we have neglected the inertia and viscosity terms, which are much smaller than the remaining term, due to the transport ordering. Using the relationship given in Eq. (7), the radial particle flux may be decomposed as

$$\begin{aligned}
\langle \boldsymbol{\Gamma}_s \cdot \nabla\psi \rangle &= -\frac{1}{e_s}\left\langle \frac{I}{B}\boldsymbol{b}\cdot(\boldsymbol{R}_s + e_s n_s \boldsymbol{E})\right\rangle \\
&\quad + \frac{1}{e_s}\left\langle \frac{\boldsymbol{B}\times\nabla\psi}{B^2}\cdot(\boldsymbol{R}_s + e_s n_s \boldsymbol{E})\right\rangle \\
&\equiv -\frac{I}{e_s\langle B^2\rangle}\left\langle B(R_{s\|} + e_s n_s E^{(A)}_\|)\right\rangle \\
&\quad - \frac{I}{e_s}\left\langle \frac{R_{s\|} + e_s n_s E^{(A)}_\|}{B}\left(1 - \frac{B^2}{\langle B^2\rangle}\right)\right\rangle \\
&\quad + \Gamma^{cl}_s + \left\langle n_s \frac{\boldsymbol{E}^{(A)}\times\boldsymbol{B}}{B^2}\cdot\nabla\psi\right\rangle \\
&= -\frac{I}{e_s\langle B^2\rangle}\left\langle \boldsymbol{B}\cdot\nabla\cdot\overleftrightarrow{\pi}_s\right\rangle \\
&\quad - \frac{I}{e_s}\left\langle \frac{R_{s\|}}{B}\left(1 - \frac{B^2}{\langle B^2\rangle}\right)\right\rangle \\
&\quad - In_s\left\langle \frac{E^{(A)}_\|}{B}\left(1 - \frac{B^2}{\langle B^2\rangle}\right)\right\rangle
\end{aligned}$$

$$+ n_s \left\langle \frac{\boldsymbol{E}^{(A)} \times \boldsymbol{B}}{B^2} \cdot \nabla\psi \right\rangle + \Gamma_s^{\mathrm{cl}}, \tag{35}$$

where we have used Eq. (23) in the final equality and implicitly assumed that n_s is the flux function. The first term in Eq. (35) is the banana-plateau flux, which is driven by the surface-averaged pressure anisotropies and is dominant in the long mean free path regime. The $E_\parallel$ component of the banana-plateau flux is associated with the Ware pinch. The second term is the Pfirsch-Schlüter flux that results from a poloidal variation of the friction force on a magnetic surface. The combination of the third and fourth terms including the electric field describes the motion of the magnetic flux surfaces [9]. When we consider the particle flux on a flux surface, these terms do not appear. The sixth term is defined as the classical flux.

In NCLASS, the flux for particles with species s and charge state i can be decomposed into banana-plateau (BP), Pfirsch-Schlüter (PS) and classical (cl) components:

$$\Gamma_{si} \equiv \langle \boldsymbol{\Gamma}_{si} \cdot \nabla\rho \rangle = \Gamma_{si}^{\mathrm{BP}} + \Gamma_{si}^{\mathrm{PS}} + \Gamma_{si}^{\mathrm{cl}},$$

where ρ denotes the flux surface. This expression is compatible with Eq. (35).

6.2 Comparison of neoclassical particle flux

In this comparison, although the amplitude of the classical flux is two orders smaller than that of the neoclassical flux, the classical flux is included in this comparison, though negligible in practice. In a concentric circular equilibrium which TASK/TX adopts, B^2 is identical to $\langle B^2 \rangle$ and, thus, the Pfirsch-Schlüter flux vanishes: the PS flux is of course finite in an actual plasma, but the magnitude is much smaller than the banana-plateau flux. In the end, we virtually compare the BP flux.

As clearly seen in Eq. (2), the radial particle flux $\Gamma_s \equiv n_s u_{sr}$ is one of the dependent variables in TASK/TX. In this sense, we do not need an analytically-reduced equation to extract the particle flux from the simulation result, unlike resistivity and the bootstrap current, as shown in Sec. 5. The neoclassical particle flux is readily obtained in TASK/TX directly by solving the set of equations with turbulent particle diffusivity set to zero. In doing so, we obtain the flux excluding the turbulence-particle flux in a simulation result in TASK/TX. A comparison of the simulation results for the electron particle flux Γ_{e}, calculated by TASK/TX and NCLASS is shown in Fig. 5 in a manner indicating that the neoclassical particle flux is accurately reproduced over the profile in the TASK/TX system, as is the case for other neoclassical properties.

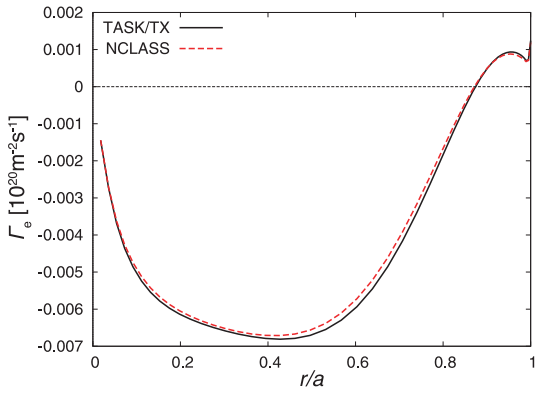

Fig. 5 Estimates from TASK/TX and NCLASS for the neoclassical particle flux.

7. Summary and Discussion

We have developed neoclassical transport modeling compatible with a system of two-fluid equations on which TASK/TX relies, with the aid of the NCLASS module. The basic idea was borrowed from the moment approach used in NCLASS as established mainly by Hirshman [9]. Considering that parallel friction acting on guiding centers is essential for neoclassical transport, we have simply introduced the parallel neoclassical viscosity tensor given in Eq. (27) into the poloidal equation of motion given in Eq. (3). Even though the neoclassical viscosities and the poloidal heat flux are estimated by NCLASS, the poloidal particle flow $u_{s\theta}$ and any other neoclassical features are self-consistently calculated solely by solving the equations in TASK/TX. Through comparisons of many important neoclassical properties with NCLASS and sometimes the Sauter model, the validity of the neoclassical modeling was confirmed.

As is usual with two-fluid equations, the chain of moment equations is truncated up to the second order moment, the energy equation, to get a closed set of equations for TASK/TX. In other words, the moment equations for heat flux are not solved in the code: instead, these equations are solved using Eq. (25) to obtain the poloidal heat flow $\hat{q}_{s\theta}$. If these equations are included in the set of equations, estimating the heat flux by solving the simultaneous equation given in Eq. (25), i.e., NCLASS, is not necessary, because $\hat{q}_{s\theta}$ becomes a dependent variable of the code. We simply have to calculate the viscosities μ_{sj} $(j = 1, 2, 3)$ based on their analytic formulae [7, 16] in terms of neoclassical transport in this case and then solve the set of equations, including the viscosity tensors given in Eqs. (21) and (22). In doing so, we enable consistent estimation of the radial heat flux (transport), similar to the particle flux shown in Sec. 6. From the standpoint of completeness of the framework of neoclassical transport theory, the code should be improved so as to solve the moment equations for heat flux and also to accommodate itself to an arbitrary equilibrium.

Acknowledgments

This work was supported by the Grant-in-Aid for Young Scientists (B) (No 22760667) from The Ministry of Education, Culture, Sports and Technology (MEXT) and

for Scientific Research (S) (No 20226017) from the Japan Society for the Promotion of Science (JSPS).

[1] M. Honda and A. Fukuyama, J. Comput. Phys. **227**, 2808 (2008).
[2] M. Honda *et al*., J. Plasma Fusion Res. SERIES **9**, 529 (2010).
[3] M. Honda *et al*., Nucl. Fusion **48**, 085003 (2008).
[4] M. Honda *et al*., Nucl. Fusion **49**, 035009 (2009).
[5] M. Honda *et al*., Nucl. Fusion **50**, 095012 (2010).
[6] A.A. Ware, Phys. Rev. Lett. **25**, 15 (1970).
[7] W.A. Houlberg *et al*., Phys. Plasmas **4**, 3230 (1997).
[8] M. Kikuchi and M. Azumi, Plasma Phys. Control. Fusion **37**, 1215 (1995).
[9] S.P. Hirshman and D.J. Sigmar, Nucl. Fusion **21**, 1079 (1981).
[10] S.P. Hirshman, Phys. Fluids **21**, 224 (1978).
[11] S.P. Hirshman, Phys. Fluids **21**, 1295 (1978).
[12] P. Helander and D.J. Sigmar, *Collisional Transport in Magnetized Plasmas* (Cambridge University Press, Cambridge, 2002).
[13] O. Sauter, C. Angioni and Y.R. Lin-Liu, Phys. Plasmas **6**, 2834 (1999).
[14] O. Sauter, C. Angioni and Y.R. Lin-Liu, Phys. Plasmas **9**, 5140 (2002).
[15] S.I. Braginskii, *Transport Processes in a Plasma*, in Rev. Mod. Phys. Vol. 1 (Consultants Bureau, New York, 1965).
[16] K.C. Shaing, M. Yokoyama, M. Wakatani and C.T. Hsu, Phys. Plasmas **3**, 965 (1996).
[17] K.C. Shaing, Phys. Fluids **31**, 2249 (1988).
[18] K. Crombé *et al*., Phys. Rev. Lett. **95**, 155003 (2005).
[19] O. Sauter, R.W. Harvey and F.L. Hinton, Contrib. Plasma Phys. **34**, 169 (1994).